Pushover Analysis and Seismic Response of UHPC Two-Column Bridge Bent

Author(s) & Affiliation: Negar Naeimi [(1)], Mohamed A. Moustafa [(1)]

[1] University of Nevada, Reno, NV, USA

Abstract:

Advanced behavior of Ultra High Performance Concrete (UHPC) is attracting a growing interest in the construction industry worldwide. Currently, UHPC is used widely in bridge deck joints and connections, while it has a great potential to be extended to larger structural applications. However, the structural behavior of UHPC for larger components is still not fully understood. The objective of this study is to better understand the overall behavior and failure mechanism of UHPC components (mainly bridge columns) using detailed finite element modeling. In particular, this paper investigates the validity of Total Strain Crack model, as a readily implemented model in DIANA FEA software, in capturing UHPC columns failure mechanism. The uniaxial behavior of UHPC in tension and compression are independently defined using the existing uniaxial stress-strain curves from the literature. The pushover response of a two-column bent of a prototype bridge with the typical geometry available in Caltrans Bridge Academy documents is studied. Besides, a reference two-column bent, of conventional concrete with the same geometry, is modeled. The reference bent is used to investigate the relative increases in strength and ductility capacities of UHPC column compared to the conventional one. Furthermore, the effect of different reinforcement ratios, steel grades and steel hardening effects on the overall behavior of UHPC columns are investigated.

Keywords: Bridges, finite element modeling, ductility index

1. Introduction

Ultra-High Performance Concrete (UHPC) is an innovative cementitious material with the exceptional high strength, performance and durability. High compression strength and low permeability of UHPC arise from finely mixed aggregates and cementitious material. Besides, high volume ratio, mostly about 2%, of high strength steel fibers with tensile strength of 200-400 ksi (1.38-2.76 GPa) leads to tensile ductility of UHPC. There is not a unique definition for UHPC. However, according to the definition of the Federal Highway Administration (FHWA) [1, 2]: *"UHPC is a cementitious composite material composed of an optimized gradation of granular constituents, a water-to-cementitious materials ratio less than 0.25, and a high percentage of discontinuous internal fiber reinforcement. The mechanical properties of UHPC include compressive strength greater than 21.7 ksi (150 MPa) and sustained post-cracking tensile strength greater than 0.72 ksi (5 MPa). UHPC has a discontinuous pore structure that reduces liquid ingress, significantly enhancing durability compared to conventional concrete."*

In the recent decades, UHPC has been used in some structures such as building components, connections and facades, bridge decks and joints, and marine structures. It has also been used for the repair and rehabilitation of damaged structures. The expanding application of UHPC in the construction industry emphasizes the need to establish specific standard guidelines for the numerical modeling and design of UHPC structures. In spite of the different material and structural behavior of UHPC compared to the conventional concrete, nonlinear analysis of many of the UHPC components are conducted using existing nonlinear constitutive models for conventional concrete due to the lack of dedicated UHPC models in the commercial software.

The brittle tensile behavior of Normal Strength Concrete (NSC), for instance, is ignored for design purposes. However, the ductile and strain hardening behavior of UHPC in tension with relatively high tensile strength is worth being considered for an optimized design. In addition, high compression strength of UHPC might require the use of higher reinforcement ratio or high strength steel to fully benefit from the superior compression strength of UHPC. The above are only few reasons why modifications to the existing design and analysis methods are vital to establish specific design codes for UHPC components. To achieve this goal, extensive experimental and numerical investigations on UHPC at both the material and structural levels, are required. This study contributes towards this goal and aims at developing a better understanding of UHPC structural behavior using 3D finite element modeling of a two-column bent of a prototype bridge. The geometry of the bent is selected from the prototype bridge available from the Caltrans Bridge Academy documents. Different reinforcement ratios and steel grade is considered to conduct comparative nonlinear pushover analysis. The main objective of the analysis is to evaluate the force and displacement capacities of UHPC bents with different reinforcement and compare these cases against a reference NSC bent.

2. Background

Previous studies on UHPC mostly focused on evaluation of the mechanical behavior of UHPC at the material level. Two reports published by FHWA comprehensively discuss the UHPC fundamental aspects [1, 3]. On the other hand, fewer studies, which used either experimental or numerical methods, investigated the structural behavior of UHPC components. It is obvious that experimental tests on large-scale UHPC columns require considerable expenses and not all the facilities can accommodate such tests. Consequently, finite element modeling, if properly validated or verified, can be a feasible solution to gain more insight into the UHPC structural design process through evaluating the structural behavior of varying UHPC components and designs. There is no predefined or dedicated constitutive model implemented in commercial software for the analysis of UHPC components yet, and many researchers have employed the existing constitutive models of conventional concrete to analyze UHPC components. For instance, Paschalis et al. [4] used the SBETA constitutive model in ATENA software for their numerical modeling. This model is not able to simulate the tension hardening behavior of UHPC and does not accurately follow the hardening and softening behavior of UHPC.

Shafieifar et. al. [5] compared the existing analytical models to predict the flexural capacity of UHPC beams. They used Concrete Damage Plasticity (CDP) model in Abaqus for their simulation [6]. In particular, the CDP model was developed for NSC modeling and is not able to simulate tensile hardening behavior of UHPC. In CDP model, the uniaxial tensile stress-strain curve follows a linear elastic relationship until the onset of micro-cracking. Beyond this point, there is a softening branch which reflects the strain localization. Yin et. al [7] used another concrete damage model, known as Karagozian & Case (K&C) model (MAT_73R3 in LS-DYNA) for their analysis. This model needs several input parameters to define the stress-strain relationship. The tensile strength and softening curve are generated from the input parameters and predefined equations for the conventional concrete with compressive strength of 45.4 MPa. Therefore, calibration of this model is vital for simulation of UHPC components, while there is still no guarantee to get the best agreement with the experimental results.

For the purpose of this study, the multi-linear Total Strain Crack model in DIANA FEA software [8] is elected and used in this study. This model has the ability to directly implement a user-defined uniaxial stress-strain relationship for both tension and compression behavior. Accordingly, stress-strain curves obtained from published UHPC material tests have been used for the total crack model input. The validity of this model and modeling approach was previously demonstrated and validated by the authors [9]. Thus, no further calibration of the constitutive model is discussed here but the implemented material behavior for the elastic, hardening and softening of UHPC in tension and compression is shown next.

3. Finite Element Modeling

In the present study, the finite element software DIANA v10.2 [8] is used for 3D modeling and analysis of the UHPC and reference NSC two-column bents. DIANA's strongest capabilities lie in nonlinear analysis for structural and concrete systems. It provides various powerful material models among other features that makes suitable for nonlinear analysis of UHPC structures. A description of the geometric model of the considered two-column bent, meshing, and details of the constitutive models are presented next.

3.1. Geometry

A typical California Bridge that is commonly used for training purposes at the Caltrans Design Academy is used in this study. This bridge is designed using conventional concrete, f'_c = 4 ksi (28 MPa) and Gr60 reinforcement, f_y = 60 ksi (420 MPa) in light of the Caltrans seismic design criteria and the recommended AASHTO LRFD Guidelines for the Seismic Design of Highway Bridges. The prototype bridge is classified as a normal bridge in seismic design category D. It is a three span prestressed reinforced concrete box girder bridge. The span lengths are 126 ft (38.4 m), 168 ft (51.2 m), and 118 ft (36.0 m). The column height varies from 44 ft (13.4 m) at Bent 2 to 47 ft (13.3 m) at Bent 3. Both bents have a skew angle of 20 deg. The columns are pinned at the bottom. For this study, the geometry of Bent 2 with columns height of 44 ft (13.4 m) and diameter of 6 ft (1.8 m) is selected (Figure 1). The columns of the prototype bridge are reinforced by 26 #14 longitudinal bars, i.e. 1.44% reinforcement ratio, and #8 hoops @ 5 in (127 mm) in the plastic hinge. A concrete cover of 2 in (51 mm) is used. The bent cap height and width are 6.75ft (2.1 m) and 8ft (2.4 m), respectively. The average column axial force from the superstructure is equal to 1694 kips (7535 kN), which corresponds to an axial load index of about 10% and 2% when NSC and UHPC are used for the columns, respectively.

3.2. Meshing

For the 3D modeling of NSC and UHPC in the two-column bent, the TP18L element from DIANA is used, which is a six-node isoparametric solid wedge element (Figure 1). It is formulated based on linear area interpolation in the triangular domain and a linear isoparametric interpolation in the ζ direction. There is a constant strain and stress distribution over the element volume. Steel bars are modeled as embedded reinforcements. Embedded reinforcements add stiffness to the finite element model. They are embedded in the structural elements, the so-called mother elements. DIANA ignores the space occupied by an embedded reinforcement. The mother element neither diminishes in stiffness, nor in weight. The reinforcement does not contribute to the weight (mass) of the element. Standard reinforcements do not have degrees of freedom of their own. The strains in the reinforcements are computed from the displacement field of the mother elements. This implies perfect bond between the reinforcement and the surrounding material. For the total crack model, the crack bandwidth, theoretically, depends on the element size, its shape, the orientation of the crack within the element, and the integration scheme. DIANA assumes a default value for the crack bandwidth h. For the solid elements, the default value is $\sqrt[3]{V}$, where V is the volume of the element. In this study, the default value is used for the crack bandwidth.

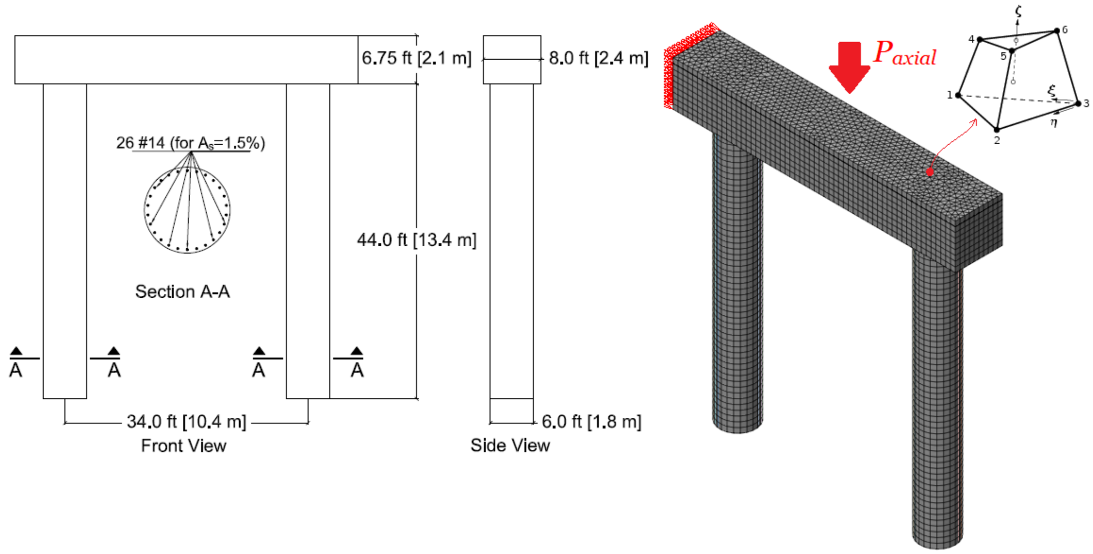

Figure 1. Geometry and finite element modeling of the two-column bent

3.3. Boundary Conditions and loading

All the elements at the column base are fixed only in the three translational directions. The nonlinear structural analysis is conducted in two phases. In the first phase, gravity load, equal to a total of 3388 kips (15070 kN) is applied in ten loading steps and distributed along all nodes at the top surface of the cap beam. A regular Newton-Raphson solver is used for the nonlinear equilibrium equations. In the second phase, a prescribed horizontal top displacement of 26.4 in (670 mm) that corresponds to 5% drift is uniformly applied to the nodes at the left section of the cap beam in 100 steps. For this phase, a secant Quasi-Newton method is used to solve the nonlinear equilibrium equations. For both phases, displacement, force, energy and residual norms are simultaneously satisfied as the convergence criteria. The load-displacement curve is generated from the base shear load versus the prescribed deformation on the left section of the bent cap.

3.4. Constitutive Model of steel rebar

In this study, steel rebars of Gr60 and Gr100 are used to evaluate the effect of reinforcing steel grade on the overall pushover behavior of the bent. For each grade of steel rebar, two different stress-stain relationships are examined and illustrated in Figure 2. Both relationships follow Von-Mises yield criterion. In the first case, stress-strain relationship is assumed to be elastic perfectly plastic. Poisson's ratio v and modulus of elasticity E are assumed to be 0.3 and 29,000 ksi (2×10^5 MPa), respectively. Yield stress f_y is assumed 60 ksi (420 MPa) for steel Gr60 and 100 ksi (690 MPa) for steel Gr100. In the second case, hardening behavior of steel is taken into account using VOCE equation as follows:

$$\sigma_y = \begin{cases} \sigma_0 + C\left(1 - e^{-\frac{\kappa - \varepsilon^{pl}}{\varepsilon^{p0}}}\right) & if \quad \kappa \geq \varepsilon^{pl} \\ \sigma_0 & if \quad \kappa < \varepsilon^{pl} \end{cases}$$

where σ_0 is the initial yield stress, c is the hardening constant, ε^{p0} is the hardening exponent and ε^{pl} is the yield plateau. Values of these four parameters are calibrated using the stress-strain relationship presented in the ACI document IGT-6R-10 for Gr60 and Gr100 steel bars.

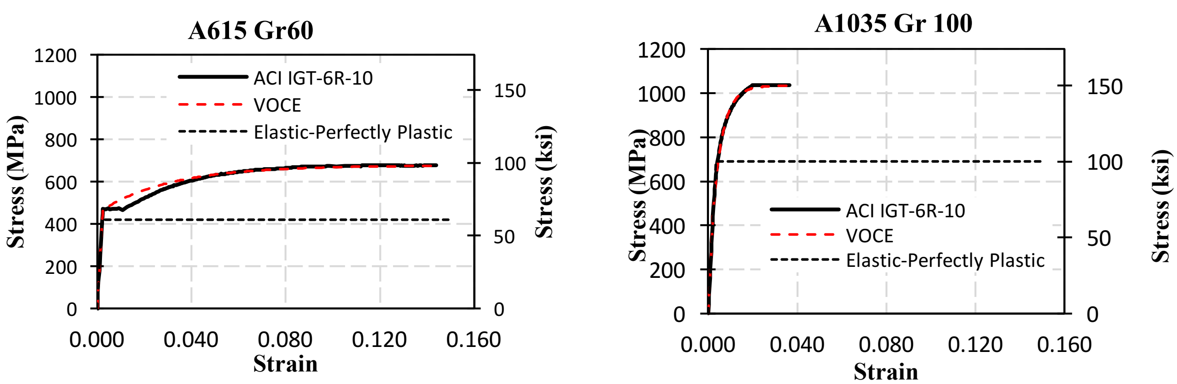

Figure 2. Stress-Strain Relationship of steel rebar (a) A615 Gr60, (b) A1035 Gr100

3.5 Constitutive Model of Concrete

The uniaxial tension and compression stress-strain curves of concrete (UHPC and NSC) are implemented in DIANA using the total strain based crack model. The total strain crack model is formulated based on the modified compression field theory of Vecchio and Collins [10]. The 3D extension to this theory is proposed by Selby and Veccio [11] to consider the lateral cracking effects. The total strain based crack models follow a smeared crack approach for the fracture energy and the coaxial stress-strain concept. In this study, the rotating crack principle is used. In the coaxial rotating crack models, cracking strains are generated by the orthogonal cracks that keep aligned with the principal directions of both strain and stress. Each crack start to open when the corresponding principle stress reaches to a critical value.

The total strain crack model, as implemented in DIANA, independently describes the tensile and compressive behavior of the material using their uniaxial stress-strain relationships. Different approaches are provided in DIANA to model each of the tensile and compressive nonlinear behavior. Among them, the multi-linear user-defined input is the best option for a new material model like UHPC, as it has the inherent potential to define any kind of stress-strain relationships, point-by-point, captured directly from experimental material tests. However, it is noted that scaling effects which reflects the differences between in-place concrete strength and cylinder compressive strength for large scale columns is not considered in the analysis. In other words, the stress-strain curves captured from the tests on UHPC small specimens is what have been directly implemented as the constitutive model without any modifications. Furthermore, due to lack of the experimental data on stress-strain relationship of UHPC cylinders confined by transverse steel reinforcement, confinement effect of spirals is not considered on UHPC.

3.5.1 Constitutive Model of UHPC

To the date, only few number of experimental programs have been carried out to obtain the full uniaxial stress-strain behavior of UHPC in tension or compression. Specifically, no extensive study has been conducted yet to capture the confined UHPC full stress-strain curve in compression. Most of the existing methods to capture the post-cracking behavior of UHPC in compression were found inefficient. For tension, it is also challenging because no relatively simple or unique test methods are codified beyond the extensive efforts done by Graybeal at the FHWA [2]. Besides, there is a controversy on the best size and shape of the specimens for the tension test. In addition to the above reasons, a wide range of materials with different mix design, ingredients, varying fiber reinforcement ratio and shape of fibers can be classified, which make a consistent constitutive model for UHPC hard to establish. For the purpose of this study, the average compression stress-strain curve captured by El-Helou [12] from tests on 12 unconfined UHPC 3×6 in (76×152 mm) cylinders, and the average tensile stress-strain curve captured by Duque and Graybeal [13] are used (Figure 3). The direct tension tests were carried out on 16 2×2×17 in (51×51×432 mm) specimens cut parallel to the UHPC flow direction in casting. All the considered specimens for both tension and compression modeling used 2% steel fibers.

3.5.2 Constitutive Model of NSC

To model the NSC, the rotating total strain crack model is used as well. Mander's Confinement equation [14] is used to determine the compression stress-strain relationship. The confined stress-strain curve is implemented by multi-linear curve in DIANA and a brittle behavior curve is assigned for the tensile stress-strain relationship of NSC as shown in Figure 3.

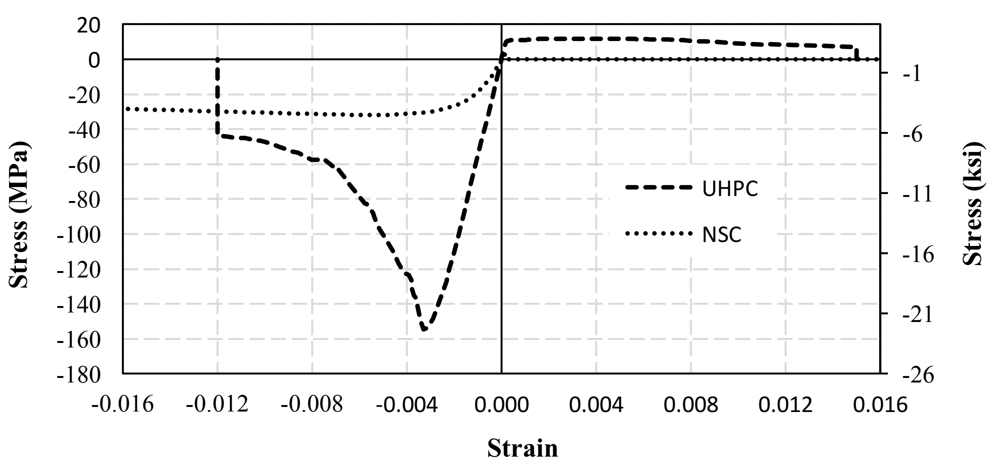

Figure 3. Stress-Strain Relationship of NSC and UHPC

4. Results and Discussion

Nonlinear structural and pushover analysis is carried out for four different cases of unconfined UHPC and one reference confined NSC bent. Table 1 summarizes the different analysis cases. For each case, three different ratios of longitudinal reinforcement is considered, As = 1.5%, 3.0% and 4.0%. The load-drift pushover curves of the UHPC bents are illustrated in Figures 4a to 4d. In each figure, every curve corresponds to a specific ratio of longitudinal reinforcement. These figures apparently reveal that the UHPC bents, when compared to the confined NSC bent, show a significantly enhanced load and displacement capacities. Comparing the UHPC and NSC bents at the section levels of the columns, higher compressive strength of UHPC provokes higher tensile load to balance. Therefore, considerable part of the UHPC column section goes under tensile stress. This large area of UHPC under tension with tensile strength of about 1.7 ksi (12 MPa), add significant flexural strength to the section. The load-drift behavior of the NSC reference bent is illustrated in Figure 4e. In Table 2, the analysis results including the maximum base shear force V_{max} and the displacement ductility μ are presented. V_{max}/V_{ref} and μ/μ_{ref} are respectively the ratio of V_{max} and μ to the V_{max} and μ of reference NSC column, for each case. Based on this table, the use of 4% ratio of Gr100 longitudinal reinforcement, considering its hardening effects, improves the ultimate load by 7.25 times of the reference NSC bent with 1.5% of Gr60 longitudinal reinforcement, which is a huge increase and motivates future experimental tests for verification.

Table 1. Summary of pushover analysis cases

Analysis case	Type of Concrete	Steel Grade	Steel stress-strain relationship
UHPC Case 1	Unconfined UHPC	Gr60	Elastic-Perfectly plastic
UHPC Case 2	Unconfined UHPC	Gr60	VOCE equation
UHPC Case 3	Unconfined UHPC	Gr100	Elastic-Perfectly plastic
UHPC Case 4	Unconfined UHPC	Gr100	VOCE equation
NSC Case 1	Confined NSC	Gr60	Elastic-Perfectly plastic

Table 2. Summary of all analysis results

Analysis case	A_s	V_{max}		V_{max}/V_{ref}	μ	μ/μ_{ref}
		kips	kN			
UHPC Case 1	1.5%	2,195	9,764	3.93	2.42	1.11
	3.0%	2,728	12,135	4.89	2.45	1.13
	4.0%	3,055	13,589	5.48	2.65	1.22
UHPC Case 2	1.5%	2,295	10,209	4.11	2.42	1.11
	3.0%	2,902	12,909	5.20	3.04	1.40
	4.0%	3,331	14,817	5.97	3.11	1.43
UHPC Case 3	1.5%	2,547	11,330	4.56	2.35	1.08
	3.0%	3,372	14,999	6.04	2.50	1.15
	4.0%	3,906	17,375	7.00	2.55	1.18
UHPC Case 4	1.5%	2,621	11,659	4.70	2.69	1.24
	3.0%	3,527	15,689	6.32	3.71	1.71
	4.0%	4,045	17,993	7.25	5.40	2.49
NSC	1.5%	558	2,482	1.00	2.17	1.00

Based on Figure 4 and Table 2 above, there are different parameters which control the pushover curve, i.e. force and displacement capacities of the two-column bent. The selected constitutive model for the steel bars is one of the factors. Comparing the results of UHPC case 1 with UHPC case 2, and UHPC case 3 with UHPC case 4, shows that considering hardening effect of steel rebars leads to higher peak strength and ductility. The increase is noticeable in ductility but can be insignificant in load capacity. Another factor is the ratio of longitudinal reinforcement.

The increase in the longitudinal reinforcement ratio results in the increase of load and displacement capacity. Effect of higher steel grade is also similar to the effect of higher reinforcement ratios. For a specific reinforcement ratio like A_s = 4.0%, V_{max} is equal to 3,331 kips (14,817 kN), for UHPC case 2, while this is 4,045 kips for UHPC case 4 (17,993 kN).

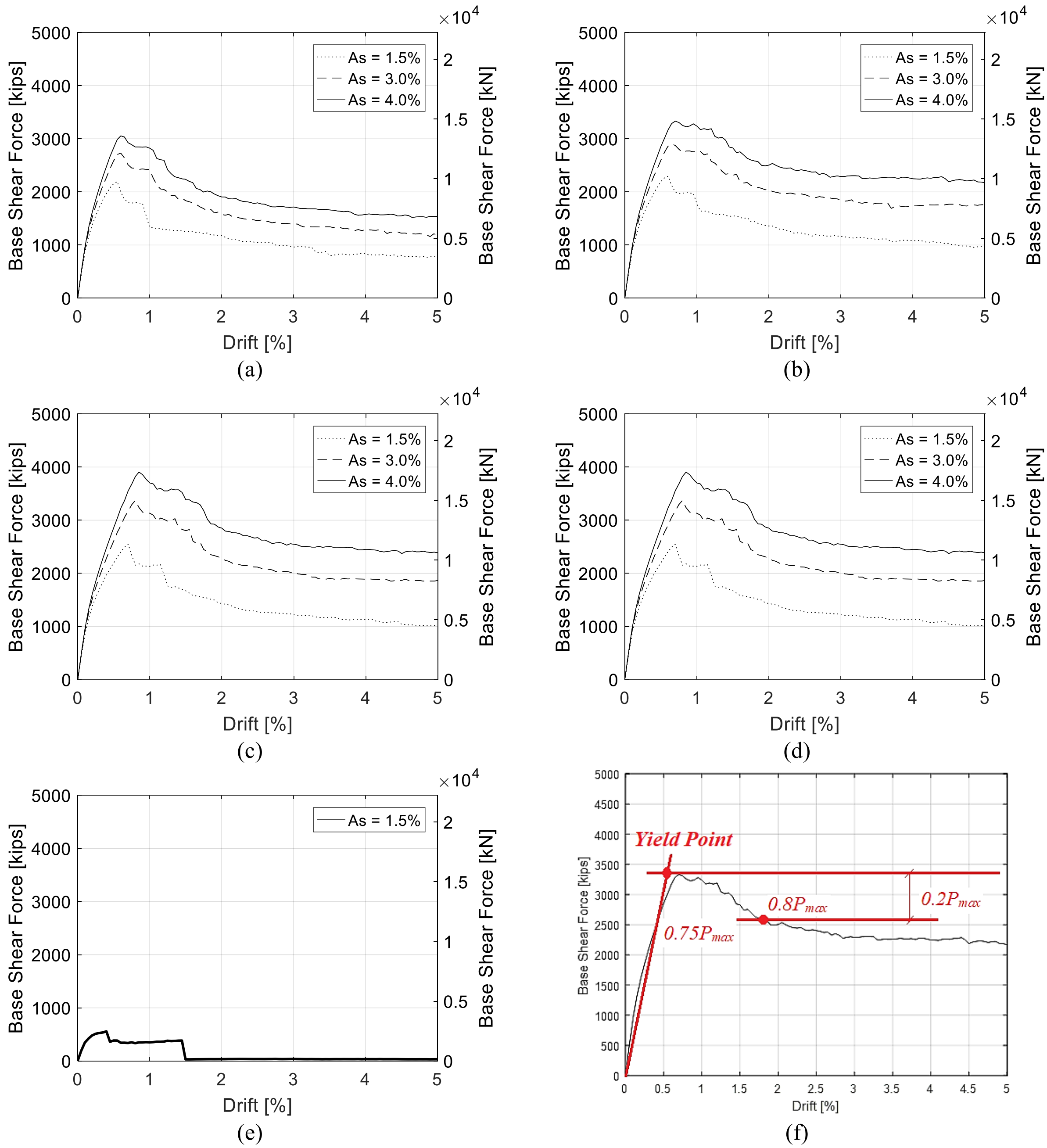

Figure 4. Load-drift (pushover) curves for UHPC: (a) case 1, (b) case 2, (c) case 3, (d) case 4, and (e) NSC; and (f) definition of displacement ductility used for results interpretation

It is noted that for defining the ductility index presented above, displacement ductility ratio is defined as the ratio of maximum displacement to the yield displacement under incrementally increasing lateral displacement [15]. Since the member yield point depends on the different factors such as stress-strain characteristics of concrete and steel, section geometry and reinforcement arrangements, it is difficult to be clearly determined. Therefore, a graphical approach is used as illustrated in Figure 4f. As shown in the figure, the intersection of the two lines corresponds to the reference yield point. The horizontal line is drawn at the maximum load level. The other line connects the origin to the point of 75% of the maximum load. The maximum displacement is the displacement beyond which strength decays more than 20% of the maximum load.

5. Summary and Conclusions

In this study, several parameters that affect the force and deformation capacities of a prototype UHPC two-column bent were numerically investigated. The numerical results were compared with the results from the analysis of reference confined NSC bent. The 3D finite element model was developed in DIANA FEA software and pushover analysis was conducted. The multi-linear total strain crack model was utilized to implement the actual tension and compression UHPC stress-strain curves. These curves, which were captured separately from tension and compression tests on UHPC specimens of 2% steel fibers, are available in the literature.

Based on the finite element analysis, UHPC bents feature a ductile behavior which is required for seismic applications. The application of UHPC rather than confined NSC can significantly increases the load and displacement capacities of the prototype two-column bent by several times that vary from 3 to 7 times. Higher ratio of the longitudinal reinforcement and higher steel grades do not necessarily lead to over-reinforced sections with brittle behavior, but rather lead to a significant enhancement in the load and displacement capacities of the bent. Therefore, it is recommended for future UHPC designs to employ higher steel reinforcement (grade and amount) for the longitudinal reinforcement to take advantage of the superior compression strength and tension contribution of UHPC.

Another potential enhancement in the UHPC strength and ductility can be demonstrated if confinement effects of steel spirals are properly accounted for. Hence, compression tests on confined UHPC specimens by steel spirals are recommended and the authors are currently conducting such tests.

6. References

[1] Haber, Z. B., De la Varga, I., Graybeal, B. A., Nakashoji, B. and El-Helou, R., "Properties and behavior of UHPC-class materials", FHWA, U.S. Department of Transportation, Report No. FHWA-HRT-18-036, 2018.

[2] Graybeal, B. A., "Design and Construction of Field-Cast UHPC Connections", FHWA, U.S. Department of Transportation, Report No. FHWA-HRT-14- 084, 2014.

[3] Graybeal, B.A., "Material Property Characterization of Ultra-High Performance Concrete", FHWA, U.S. Department of Transportation, Report No. FHWA-HRT-06-103, 2006.

[4] Paschalis S.A., Lampropoulos A.P. and Tsioulou O., "Experimental and numerical study of the performance of ultra high performance fiber reinforced concrete for the flexural strengthening of full scale reinforced concrete members", Constr. Build. Mater., Vol. 186, 2018, pp. 351–366.

[5] Shafieifar M., Farzad M. and Azizinamini A., "A comparison of existing analytical methods to predict the flexural capacity of Ultra High Performance Concrete (UHPC) beams", Constr. Build. Mater., Vo. 172, 2018, pp.10–18.

[6] Shafieifar M., Farzad M. and Azizinamini A., “Experimental and numerical study on mechanical properties of Ultra High Performance Concrete (UHPC)”, Constr. Build. Mater., Vol. 156, 2017, pp. 402–411.

[7] Yin H., Shirai K. and Teo W., “Numerical Assessment of Ultra-high Performance Concrete Material”, IOP Conf. Ser.: Mater. Sci. Eng., Vol. 241, 2017, pp. 12004.

[8] DIANA, FEA. "Diana User’s Manual, Release 10.1." DIANA FEA BV, 2017.

[9] Naeimi, N. and Moustafa, M.A. “Three-Dimensional Finite Element Modeling of UHPC Using Total Strain Crack Models”, AFGC-ACI-fib-RILEM Int. Symposium on Ultra-High Performance Fibre-Reinforced Concrete, UHPFRC 2017, October 2-4, 2017, Montpellier, France.

[10] Vecchio F. J. and Collins, M. P., “The Modified Compression-Field Theory for Reinforced Concrete Elements Subjected to Shear”, J. of the American Concrete Inst., vol. 83, 1986, pp 219-231.

[11] Selby, R.G. and Vecchio F. J. “Three-dimensional constitutive relations for reinforced concrete”, 1995.

[12] El Helou, R. G., “Multiscale Computational Framework for Analysis and Design of Ultra-High Performance Concrete Structural Components and Systems”, 2016.

[13] Duque, M. L. F. and Graybeal, B. “Fiber orientation distribution and tensile mechanical response in UHPFRC”, Mater Struct, Vol. 50, No. 1, 2016, pp 55.

[14] Mander, J. B., Priestley, M. J. N. and Park, R., “Theoretical Stress- Strain Model for Confined Concrete”, J. Struct. Eng., Vol. 114, No. 8, 1988, pp. 1804–1826.

[15] Saatcioglu M., “Deformability of Reinforced Concrete Columns”, Spec Publ, Vol. 127, 1991, pp. 421–52.